

# T cell receptor antagonism interferes with MHC clustering and integrin patterning during immunological synapse formation

Cenk Sumen,<sup>1,2</sup> Michael L. Dustin,<sup>3,4</sup> and Mark M. Davis<sup>1,2</sup>

<sup>1</sup>Howard Hughes Medical Institute and <sup>2</sup>Department of Microbiology and Immunology, Stanford University School of Medicine, Stanford, CA 94305

<sup>3</sup>Department of Pathology and <sup>4</sup>Skirball Institute of Biomolecular Medicine, New York University School of Medicine, New York, NY 10016

**T** cell activation by nonself peptide–major histocompatibility complex (MHC) antigenic complexes can be blocked by particular sequence variants in a process termed T cell receptor antagonism. The inhibition mechanism is not understood, although such variants are encountered in viral infections and may aid immune evasion. Here, we study the effect of antagonist peptides on immunological synapse formation by T cells. This cellular communication process features early integrin engagement and T cell motility arrest, referred to as the “stop signal.” We find that synapses

formed on membranes presenting antagonist–agonist complexes display reduced MHC density, which leads to reduced T cell proliferation that is not overcome by the costimulatory ligands CD48 and B7-1. Most T cells fail to arrest and crawl slowly with a dense ICAM-1 crescent at the leading edge. Similar aberrant patterns of LFA-1/ICAM-1 engagement in live T–B couples correlate with reduced calcium flux and IL-2 secretion. Hence, antagonist peptides selectively disable MHC clustering and the stop signal, whereas LFA-1 valency up-regulation occurs normally.

## Introduction

At the heart of the adaptive immune response lies the ability of T cells to recognize processed foreign antigens. T cell activation is initiated and restricted by the cell surface binding of peptide–major histocompatibility complex (pMHC) ligands by the T cell receptor (TCR; Davis et al., 1998). Framed by the engagement of adhesion molecules such as CD2/CD48 and LFA-1/ICAM-1, the TCR is phosphorylated by Src-family kinases such as Lck and Fyn, which allows the docking of downstream effectors such as ZAP-70, LAT, SLP-76, and PLC- $\gamma$ , and subsequent signaling cascades that stimulate the T cell to divide, differentiate, and express proteins that ultimately guide the cells of the immune response (Dustin and Chan, 2000). Costimulatory molecules such as CD28/CD80 and CD40L/CD40 interact rapidly after ini-

tial TCR triggering. This process is sensitive to the kinetic parameters that govern TCR–pMHC complex formation (Matsui et al., 1994; Lyons et al., 1996; Kersh et al., 1998), but other factors, such as pMHC stability (Holler and Kranz, 2003) or large changes in heat capacity, (Krogsgaard et al., 2003) can also play a role.

Altered peptide ligands (APLs) are variants of wild-type TCR-activating peptides that produce a range of effects from differential cytokine production to null peptides with no activity (Sloan-Lancaster and Allen, 1996). Antagonist peptides are a rare subset of APL that block T cell activation to otherwise stimulatory concentrations of agonist ligand (De Magistris et al., 1992; Sloan-Lancaster et al., 1994). In general, antagonist ligands have lower affinities and faster off-rates for a given TCR than agonists (Lyons et al., 1996; Wu et al., 2002), with some exceptions (Sykulev et al., 1998). Structural studies have indicated that in at least one

The online version of this article includes supplemental material.

Address correspondence to M.M. Davis, Dept. of Microbiology and Immunology, Stanford University School of Medicine, 279 Campus Dr., Beckman Center, B 221, Stanford, CA 94305. Tel.: (650) 725-4755. Fax: (650) 723-1399. email: mdavis@cmgm.stanford.edu

C. Sumen's present address is The Center for Blood Research Institute for Biomedical Research, Harvard Medical School, Boston, MA 02115.

Key words: lymphocyte activation; macromolecular systems; three-dimensional imaging; T cell receptor; cell communication

Abbreviations used in this paper: APC, antigen-presenting cell; APL, altered peptide ligand; cSMAC, central supramolecular activation complex; GPI, glycosyl-phosphatidyl inositol; IRM, interference reflection microscopy; MCC, moth cytochrome  $c$ ; pMHC, peptide–major histocompatibility complex; pSMAC; peripheral supramolecular activation complex; TCR, T cell receptor.

case, the poor affinity of an antagonist ligand can be explained by a packing defect in its association with TCR when complexed to MHC (Baker et al., 2000). The filling of this space increases the affinity and is sufficient to revert the peptide into an agonist. Antagonist pMHC complexes usually need to be in excess of activating (agonist) pMHC complexes on the antigen-presenting cell (APC) surface to block T cell activation, although there are exceptions, notably in the class I MHC/CD8<sup>+</sup> T cell system (Purbhoo et al., 1998; Sykulev et al., 1998). Antagonist peptides clearly have physiological relevance, as some pathogens may use antagonist peptide mutants of dominant MHC epitopes to hinder the T cell response during the course of infection. Such antagonist variant epitopes are thought to play a role in HIV and HBV viral modulation of T cell immunity (Bertolotti et al., 1994; Klenerman et al., 1994; Purbhoo et al., 1998).

Recently, it has been found that T cell activation occurs in the context of a highly organized membrane junction between the T cell and the APC termed the immunological synapse (Monks et al., 1998; Grakoui et al., 1999). The hallmarks of a mature synapse are binding and transport of pMHC complexes into the central supramolecular activation complex (cSMAC), surrounded by a more extensive integrin-rich region, the peripheral supramolecular activation complex (pSMAC; Bromley et al., 2001a). Integrins link cytoskeletal rearrangement and cell adhesion to engagement of extracellular matrix or cell surface ligands. As adhesion precedes mature synapse formation, integrins serve an indispensable function in the formation of the immunological synapse (Dustin and Chan, 2000). LFA-1 ( $\alpha$ L $\beta$ 2) is arguably the most important integrin for leukocyte function, regulating T cell activation and contact formation via interactions with its cell surface ligands ICAM-1, -2, or -3. TCR signaling causes an increase in the affinity/avidity/valency of LFA-1 for its ligands, through an “inside-out” signaling process involving differential cytoskeletal association and ligand induced conformational changes (Kucik et al., 1996; Takagi et al., 2002; Kim et al., 2003). Signaling through LFA-1 also aids synapse formation by synergizing with CD28 in triggering the active transport of TCR/CD3 to the cSMAC in activated (Wulfing and Davis, 1998; Wulfing et al., 2002), but not naive, T cells (Bromley and Dustin, 2002). Lastly, integrin engagement (“outside-in”) along with signals downstream of the TCR complex serve to modulate the cessation of T cell migration upon activation, collectively termed the “stop signal” (Dustin et al., 1997; Dustin, 2002). Correlating with a mature synapse pattern, the stop signal arises from Ca<sup>2+</sup>-dependent arrest of cell motility and down-modulation of myosin motor function as well as T cell cytoskeletal remodeling that stabilizes the cell–cell interface, allowing a long-lived contact and continuous TCR-driven signaling (Dustin, 2003; Huppa et al., 2003; Jacobelli et al., 2004). Hence, as corroborated by *in vivo* intravital imaging in mouse lymph nodes, antigen recognition on activated dendritic cells by naive T cells leads to stable contact formation concurrent with cytokine production (Mempel et al., 2004).

Here, we characterize the effects of TCR antagonism on the formation of the immunological synapse, using both a supported lipid bilayer system and live B cells to present

pMHC complexes. Simultaneous presentation of antagonist and agonist peptide-loaded MHC molecules in the presence of integrin ligands reduces T cell adhesion to membranes at limiting antigen concentration. Although a similar fraction of adherent T cells are able to cluster MHC, the density of MHC in the cSMAC is significantly reduced in the antagonized contacts compared with the null peptide control. This decrease correlates with a block in T cell proliferation that is not rescued by incorporation of the costimulatory ligands B7-1 and CD48 into the bilayer. For the majority of T cells unable to stop and form a stable contact, integrin engagement as monitored by ICAM-1 accumulation occurs in a unique crescent-shaped pattern at the leading edge. Surprisingly, the density of integrin ligand in these moving contacts is equivalent to that of pSMAC-localized integrins in a mature, stable synapse, suggesting that up-regulation of LFA-1 binding to ICAM-1 does occur but is not sufficient for T cell arrest in the bilayer system. We extend these findings to live three-dimensional imaging of the T–B cell interface and demonstrate that copresentation of antagonist and agonist pMHCs invokes similar ICAM-1 accumulation patterns, although these T cells maintain contact with the B cell surface. Nonetheless, antagonist pMHCs compromise downstream effector functions such as elevated intracellular Ca<sup>2+</sup> and IL-2 secretion. Hence, TCR antagonists hinder synapse formation by attenuating the stop signal but not integrin activation, manifested as a dense sickle-like pattern of integrin ligand engagement. In addition, antagonists decrease pMHC transport to the cSMAC in the contacts that can overcome this effect, which may be the result of direct competition for TCR binding while lacking sufficient interaction for complete signaling.

## Results

### TCR antagonism and MHC cluster density

To model the interaction of a CD4<sup>+</sup> effector T cell encountering an APC with a mixture of activating and antagonistic peptides on its surface, we used a planar bilayer system presenting a fixed density of glycosyl-phosphatidyl inositol (GPI) linked class II MHC I-E<sup>k</sup> (100 per square micron, 20% peptide loading), containing a mixture of wild-type moth cytochrome *c* (MCC; 88–103) and either of the single amino acid peptide mutants K99R (antagonist) or K99A (null). These APLs bind MHC as well as the wild-type MCC peptide and were used to represent their functional class throughout this study. The same peptide concentrations were used at all times (10  $\mu$ M, optimal for MHC loading) to generate the same pMHC densities in order to avoid variation in pMHC complex formation. At a 1:10 dilution of MCC into 10  $\mu$ M of total peptide, the density of agonist/MHC achieved on the bilayer (10 molecules per square micron) was well within the threshold required to arrest T cell migration and to trigger synapse formation, as similar fractions of cells adhered tightly to the bilayer for both APLs (Fig. 1 a). Likewise, a comparable subset of cells accumulated MHC in the synapse for both the 99R and 99A peptide mixtures (Fig. 1 a). At a 1:100 dilution of MCC, the agonist/MHC density (1 per square micron) was near the threshold of detection for this system (Grakoui et al., 1999;

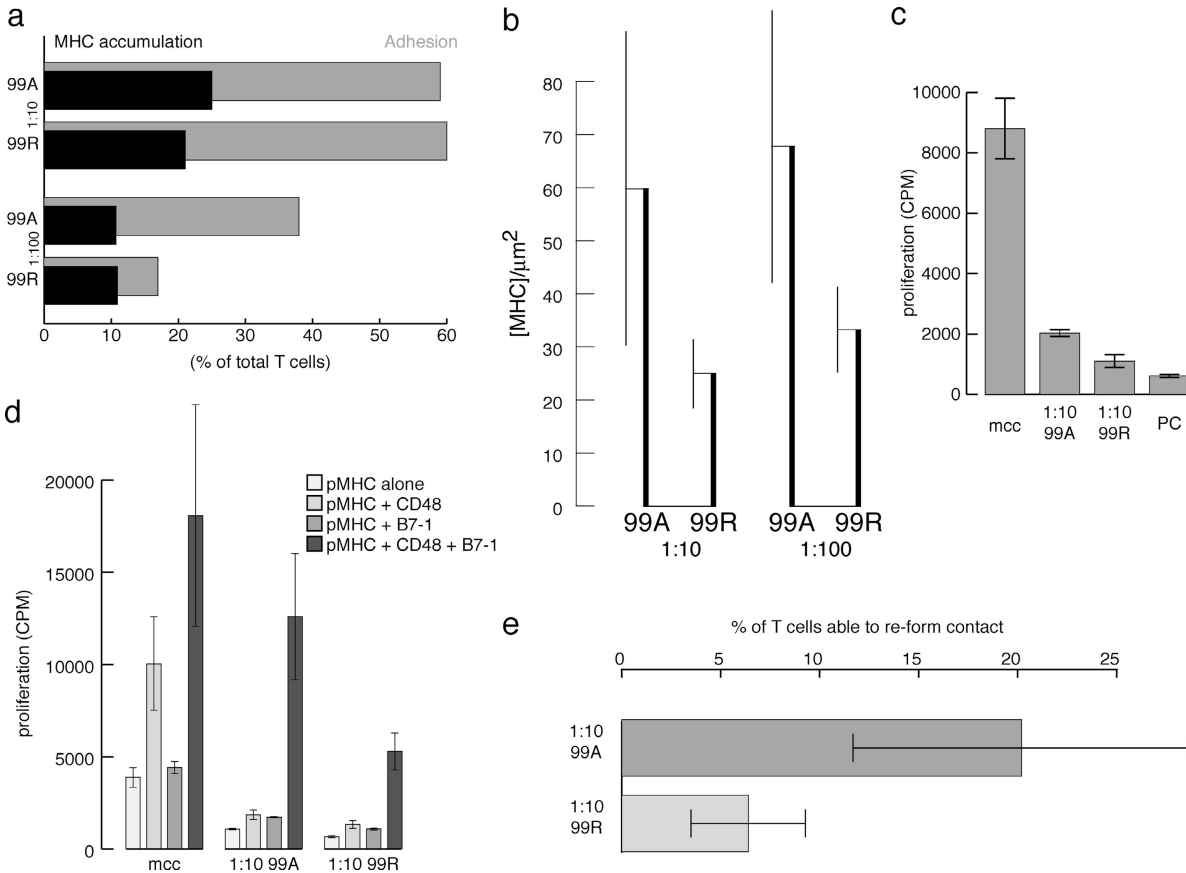


**Figure 1. Adhesion and MHC accumulation at limiting agonist concentrations.** (a) T cell adhesion to bilayers presenting agonist and APL. Primed 5C.C7 T cells were incubated with membranes containing ICAM and MHC in a parallel-plate flow chamber. The MHC was loaded with MCC agonist and excess APL, either a null peptide (99A) or an antagonist (99R). After 30 min, the ratio of input cells that formed tight interfaces (average synapse area  $\sim 50 \mu\text{m}^2$ ) as judged by IRM (adhesion, gray bars) and those that could cluster MHC (black bars) were scored. (b) Antagonists reduce MHC density in the cSMAC. From the subset of T cells that accumulated MHC, the cluster density was quantified (Grakoui et al., 1999). Both pairwise comparisons are  $P < 0.01$  by *t* test. (c) Antagonists reduce T cell proliferation. A bilayer with no protein (PC) was included as a negative control. Error bars represent average of two independent experiments normalized to the same MHC density. The difference between 99A and 99R is significant with  $P < 0.05$  by *t* test. (d) CD2 and CD28 ligands do not overcome TCR antagonism. Density of molecules on bilayer are as follows: MHC, 100 per square micron (10% peptide loaded); CD48, 175 per square micron; B7-1, 175 per square micron. (e) Antagonized T cells are unable to reform contacts upon disruption. T cells in contact with the bilayer for  $\sim 1$  h are then induced to detach over 2–5 min with a pulse of cold buffer. The ratio of cells able to reform contacts within 30 min is scored. ( $n > 200$  cells,  $P < 0.001$ ). Note that the ratio of T cells that initially adhere is similar for the two peptide mixtures (a, adhesion at 1:10 dilution). Results are representative of three experiments.

Bromley et al., 2001b). Even though the fraction of cells that formed an MHC cluster was once again similar, less than half as many T cells could adhere and form a tight contact with the bilayer containing excess antagonist peptide compared with control null peptide (Fig. 1 a, 17% vs. 38%). From the subset of these cells that accumulated MHC, we quantified the density of MHC in the central cluster. Throughout the entire range of dilutions of agonist into excess antagonist peptide 99R, there was a significant decrease (to below 50 per square micron) in the density of MHC clustered in the synapse as compared with excess null peptide 99A (Fig. 1 b).

The equilibrium MHC cluster density has been shown to directly correlate with the extent of T cell activation (Grakoui et al., 1999). As predicted, the lower cluster density of MHC in the single cell contacts affected by antagonist pMHCs caused a significant decrease in T cell prolifer-

ation (Fig. 1 c). Addition of the extracellular domains of the costimulatory ligands B7-1 and CD48 to the bilayer as purified GPI-linked molecules augmented proliferation but did not overcome the antagonism effect (Fig. 1 d), which is consistent with experiments using T cells and APC, which express these ligands at comparable densities (Sloan-Lancaster and Allen, 1996). CD2-CD48 engagement did increase T cell activation at these ligand densities, in accord with a recent report (Zaru et al., 2002). We also noticed a synergistic effect of CD48 and B7-1 in increasing T cell proliferation, with a concomitant change in their accumulation patterns when both were present (unpublished data). These primed “effector” CD4+ T cells were fairly insensitive to B7-1 in the absence of CD48, in marked contrast to naive T cell activation with planar membranes (Bromley et al., 2001b). In summary, antagonist peptides in excess over agonists can cause a decrease in MHC den-

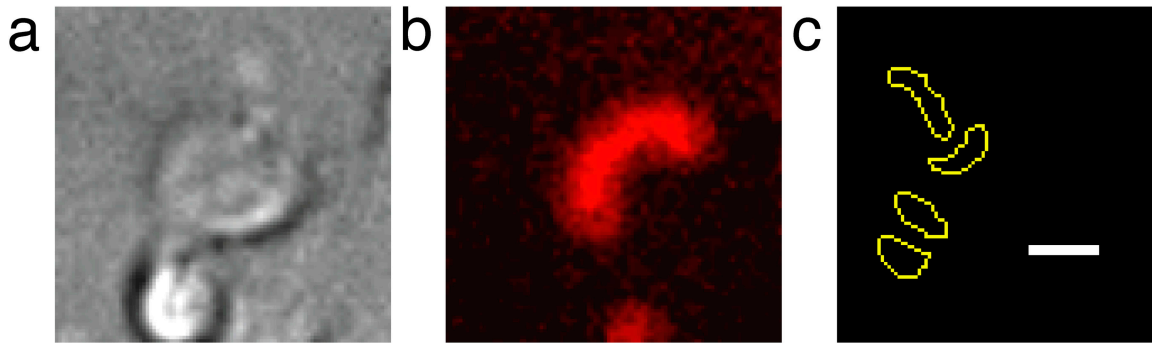


**Figure 2. Antagonist peptide complexes in the presence of agonist can cause a distinct ICAM-1 accumulation pattern.** Primed 5C.C7 T cells were exposed to bilayers containing MHC loaded with MCC agonist and antagonist peptides. The brightfield (dic) (a) and ICAM-1 fluorescence (b) panels are of a T cell representative of this “sickle-like” phenotype on a bilayer with 1:2 ratio of agonist/antagonist; more T cells formed this pattern at higher ratios of antagonist versus agonist (provided agonist density was within limits of T cell sensitivity). Higher agonist density, with the excess antagonist present, also led to more ICAM-1 sickles and the associated crawling behavior (see Video 1). This ICAM-1 shape was rarely seen with agonist diluted into other (null) APLs (e.g., at this ratio, 84% of contacting cells on an antagonist-agonist bilayer showed the sickle phenotype, whereas with the same ratio of null peptide only 12% showed this shape, consistent with the 13% crescent-shaped accumulations reported by Somersalo et al. [2004] with human CD8+ T cells in the absence of TCR agonists on the bilayer). T cells migrated rapidly in arc-shaped paths toward the ICAM-1 accumulation and away from the point of contact, as depicted in panel c. Each yellow trace, beginning with contact at top left, outlines the ICAM-1 accumulation of the same T cell at 4-min intervals. Bar, 10  $\mu\text{m}$ . ICAM, 225 per square micron; MHC, 350 per square micron. Results are representative of at least five experiments.

sity in the immunological synapse, together with a significant decrease in T cell activation.

#### Readhesion blocked by antagonism

TCR antagonism is thought to create an anergic state that renders the T cell unable to respond to antigen for up to several days following exposure to antagonist peptides (Sloan-Lancaster and Allen, 1996). To investigate anergy in our system, we took advantage of our previous observation that formation of a tight interface between bilayer and T cell observable by interference reflection microscopy (IRM) is highly dependent on productive TCR signaling (Grakoui et al., 1999). After allowing T cells to adhere to bilayers with 1:10 dilutions of MCC into the APL in a flow chamber, we disrupted the contacts by pulsing with cold buffer, which causes gradual detachment of the cell from the bilayer membrane. The temperature was then returned to 37°C and the T cells were scored using IRM for the ability to reform tight contacts. When we compared T cell contact reinitiation on bilayers where either antagonist (99R) peptide or the null (99A) variant were combined with agonist, we saw a significant decrease in the percentage of T cells that were able to reestablish tight contact (Fig. 1 e, 6.4% vs. 20.2%, respectively). It is important to note that initial adhesion rates for the two conditions at this peptide dilution were very similar (Fig. 1 a, adhesion at 1:10 was 60% vs. 59%). This refractory state lasted for at least half an hour. Hence, T cells were inhibited from activation, at least with respect to adherence and synapse formation, by prior exposure to a mixture of agonist and antagonist ligands.

We have recently shown that the “null” peptide MCC99A, although having no biological activity on its own, can nevertheless participate in agonist-driven MHC clustering and augment T cell activation at low MHC densities (Wulfing et al., 2002). The bilayer experiments described here are at higher densities where this synergistic effect has not been ob-

served. Nevertheless, to rule out that the deleterious effects of 99R compared with 99A on T cell activation is not simply a result of the loss of this property of 99A, we have also made comparisons with 99E, another MCC variant that forms a pMHC complex that does not contribute in any detectable manner to synapse formation or activation (Wulfing et al., 2002). We found that 99R still displayed antagonism when compared with 99E (Fig. S1, available at <http://www.jcb.org/cgi/content/full/jcb.200404059/DC1>), which is consistent with previous results (Rabinowitz et al., 1996).

#### Unique ICAM-1 engagement pattern during TCR antagonism

Studying the patterns of GPI-linked ICAM-1 accumulation in the presence of antagonist peptides, among the majority of T cells that were unable to form a bona fide synapse with MHC accumulation, we noticed a prominent crescent- or sickle-like accumulation of ICAM-1 (Fig. 2, a and b). This phenotype predominated at higher agonist pMHC densities while maintaining excess antagonist, and was clearly different than the patterns of ICAM-1 on bilayers without agonist or with antagonist pMHC alone (Grakoui et al., 1999), but was similar to ICAM-1 engagement in mobile contacts formed by ionomycin-energized Th1 cells (Heissmeyer et al., 2004). Cells with this aberrant integrin accumulation did not stop and reorient toward the bilayer, but slowly crawled ( $3 \mu\text{m}/\text{min} \pm 0.7 \mu\text{m}$ ) in the direction of the polarized ICAM-1 sickle. Their migration paths resembled long alternating arcs ( $r = 15 \mu\text{m}$ ) directed away from the site of initial contact (Fig. 2 c). LFA-1 on the T cell could apparently engage and aggregate its ligand ICAM-1, despite the fact that the stop signal was blocked by TCR antagonism. Similar patterns were also observed with another antagonist variant of MCC, T102G (unpublished data). The addition of PMA, a phorbol ester that activates PKC, was unable to

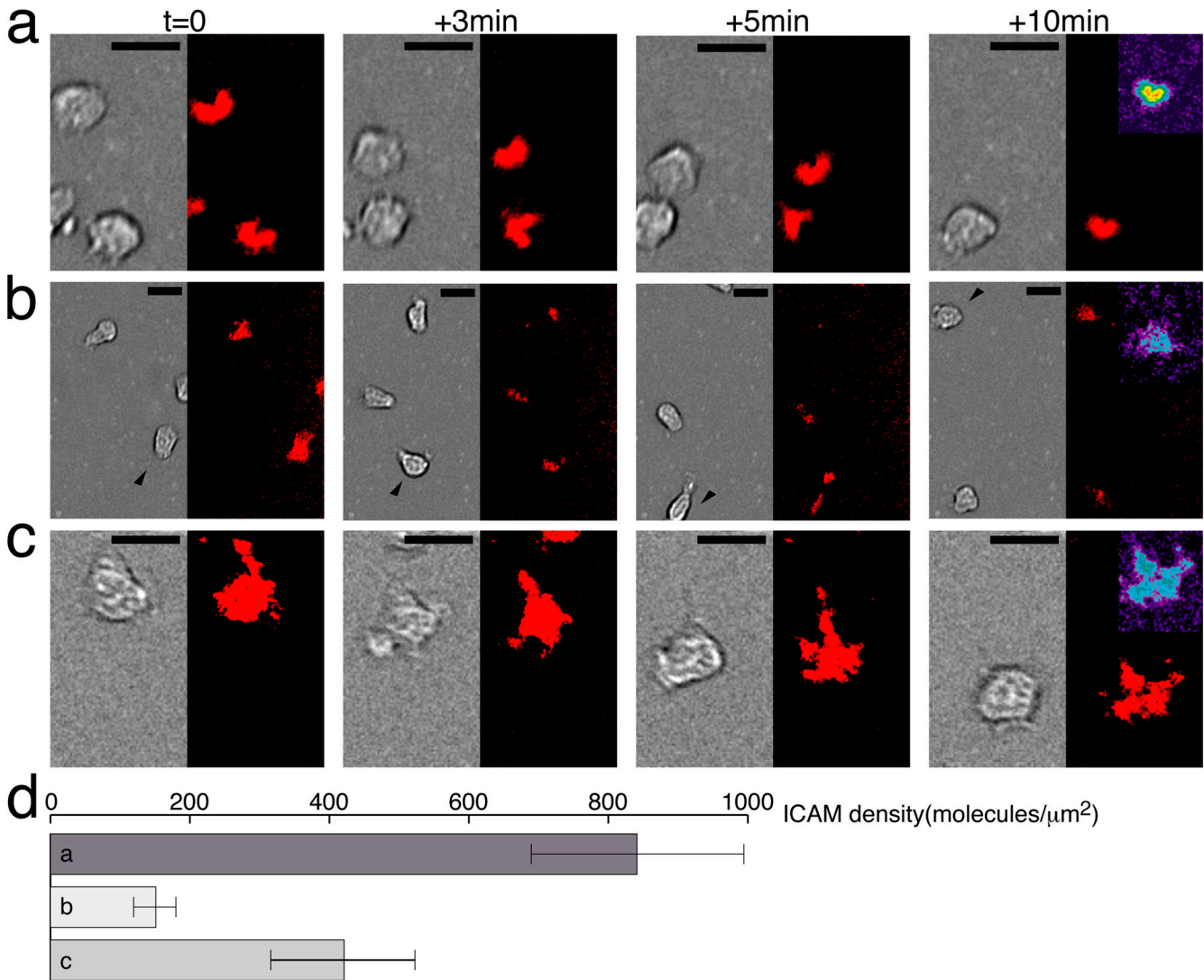


**Figure 3. Sustained interaction with antagonist-MHC affects ICAM-1 accumulation density and geometry.** (a) 5C.C7 T cell blasts were allowed to interact with bilayers expressing ICAM-1, MCC-tethered GPI-MHC ( $\alpha 32$ ) and excess 99R-loaded His-MHC complexes. ICAM-1 (red) is intensity normalized for each sequence to best demonstrate accumulation pattern. The inset in pseudocolor compares the final cluster intensity using the same scale for all three conditions. Most T cells showed the sickle-like ICAM-1 pattern and crawling pattern. (b) With no  $\alpha 32$  (antagonist-MHC alone), T cells exhibit decreased ICAM-1 clustering (left, inset; ICAM-1 density is 1/3 that in panel a) and more random crawling patterns, which is consistent with previous findings (Grakoui et al., 1999). Arrowheads denote the same T cell at the four time points. (c) After 1 h of contact, cells on the mixed TCR ligand bilayer in panel a reverted to more randomly distributed ICAM-1 patterns and lower ICAM-1 density consistent with antagonist-mediated energy. However, migration was still slowed and the cells retained close contact with the bilayer. (d) ICAM-1 density in contacts (a, 99R+MCC; b, 99R alone; c, a after 1 h), a direct indicator of LFA-1 valency. T cells from panel a were able to cluster ICAM-1 to levels as high as those forming mature synapses on agonist alone (Grakoui et al., 1999), and several-fold higher than cells on antagonist alone (b). After 1 h of contact (c), the ICAM-1 density decreased, consistent with the pattern change in ICAM engagement, indicating that the T cells could no longer respond to the agonist. Bars, 10  $\mu\text{m}$ . 99R-MHC, 750 per square micron; ICAM, 190 per square micron; MCC-MHC (a and c), 75 per square micron; MCC-MHC (b), 0. Density quantification is representative of two independent experiments.

provide the stop signal or alter the pattern of ICAM-1 accumulation (unpublished data). To further investigate this event at more optimal concentrations of agonist for T cell activation and LFA-1 up-regulation, we formed a two-component pMHC system featuring high-density mobile pMHC coupling through His-tagged MHC I-E<sup>k</sup> and NiNTA lipid derivatives, as well as lipids (GPI) covalently coupled to MHC as used here and in previous experiments (Grakoui et al., 1999). Using this new method, we could achieve mobile MHC densities of several thousand mole-

cules per square micron, which could activate T cells and cluster into synapses (unpublished data).

Using excess antagonist (99R)-loaded His-MHC on the same membrane as GPI-linked MHC with the agonist MCC peptide covalently attached to the MHC  $\alpha$  chain (referred to as  $\alpha 32$ ; Wulfing et al., 2002), we characterized T cell behavior and ICAM-1 accumulation. On these bilayers, a majority of T cells adhered and formed the sickle-shaped ICAM-1 accumulations that we had previously observed, migrating away from the point of initial membrane contact (Fig. 3 a and

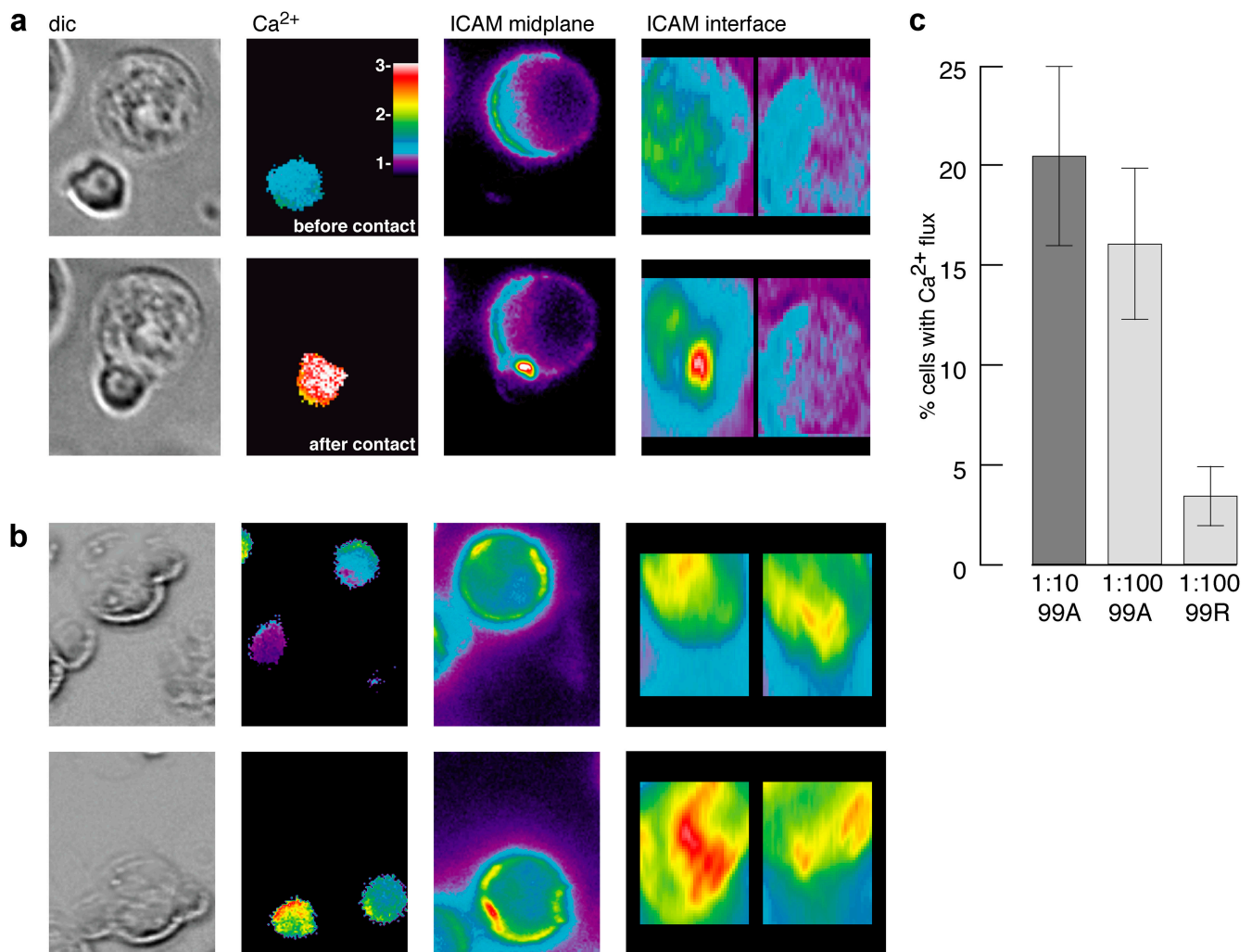


**Figure 4. ICAM-1 patterns and antagonism in live B cell-T cell couples.** 2B4 T cell blasts were incubated with CH27 B cells expressing an ICAM-GFP fusion protein (Wulfing et al., 1998). (a) When the B cells were loaded with  $10 \mu\text{M}$  MCC, consistent with previous results (Wulfing et al., 1998), the T cells showed tight contact formation, a sustained calcium flux, and an early concentrated central ICAM-1 accumulation. The first two panels show brightfield (dic) and intracellular  $Ca^{2+}$ , and the last two ICAM-1 fluorescence, with a midplane followed by a three-dimensional reconstruction panel, the first image depicting the T-B cell interface and the second another area of the B cell membrane as control. The top and bottom series show time before and after contact and the same pseudocolor scale for calcium used for all four panels is shown in the topmost panel (numbers are fold over average baseline),  $\Delta t = 60\text{s}$ . (b) At a 1:100 dilution of agonist into antagonist, most ( $\sim 60\%$ ) T cell-B cell interactions resulted in an ICAM-1 pattern similar to that seen in the bilayer system (Figs. 2 and 3). The ICAM-1 interface panels are reconstructed from a series of images at  $1\text{-}\mu\text{m}$  z-planes through the cell. In panel a, the first image shows the T cell interface as seen from the B cell side, and the adjacent image the membrane area directly opposite the T cell contact. In panel b, the T-B cell interface of the nonfluxing cell (top right) is instead shown as the control. (c) TCR antagonism correlates with decreased calcium flux: for example, the cell in panel a has about threefold higher calcium upon contact than the one in panel b. B cells loaded with the indicated peptide mixtures (all dilutions of MCC into APL) were allowed to interact with Fura-2-loaded T cells. Greater than 500 T cells were scored for elevated calcium levels.  $P < 0.01$  between 99A and 99R dilutions by  $t$  test. Results are representative of two independent experiments.

Video 1, available at <http://www.jcb.org/cgi/content/full/jcb.200404059/DC1>. Stable MHC clustering was not observed in any of these mobile contacts (unpublished data). In contrast, T cells on a bilayer with 99R-MHC (without  $\alpha 32$ ) exhibited much less efficient adhesion, with sparse ICAM-1 accumulation at the contact area (Fig. 3 b and Video 2, available at <http://www.jcb.org/cgi/content/full/jcb.200404059/DC1>). Hence, antagonist peptide itself does not elicit the sickle-shaped ICAM-1 accumulation pattern seen with a combination of agonist and antagonist ligands. Cell motility also occurred in a more random pattern, in accord with previous data of ICAM-1 engagement on bilayers presenting any

nonactivating pMHC (Grakoui et al., 1999). Consistent with the results shown in Fig. 1 e, when we imaged the bilayer in Fig. 3 a after 1 h of contact, we found that the T cells did indeed appear anergized, as defined by the loss of the sickle-shaped ICAM-1 accumulation that had formed upon initial contact (Fig. 3 c and Video 3, available at <http://www.jcb.org/cgi/content/full/jcb.200404059/DC1>). The ICAM-1 pattern after 1 h generally resembled that of T cells on antagonist alone, despite having more ICAM-1 at the interface (Fig. 3 c, right). In addition, the T cells did not break contact with the bilayer or lapse into the random crawling patterns seen without agonist peptide present.

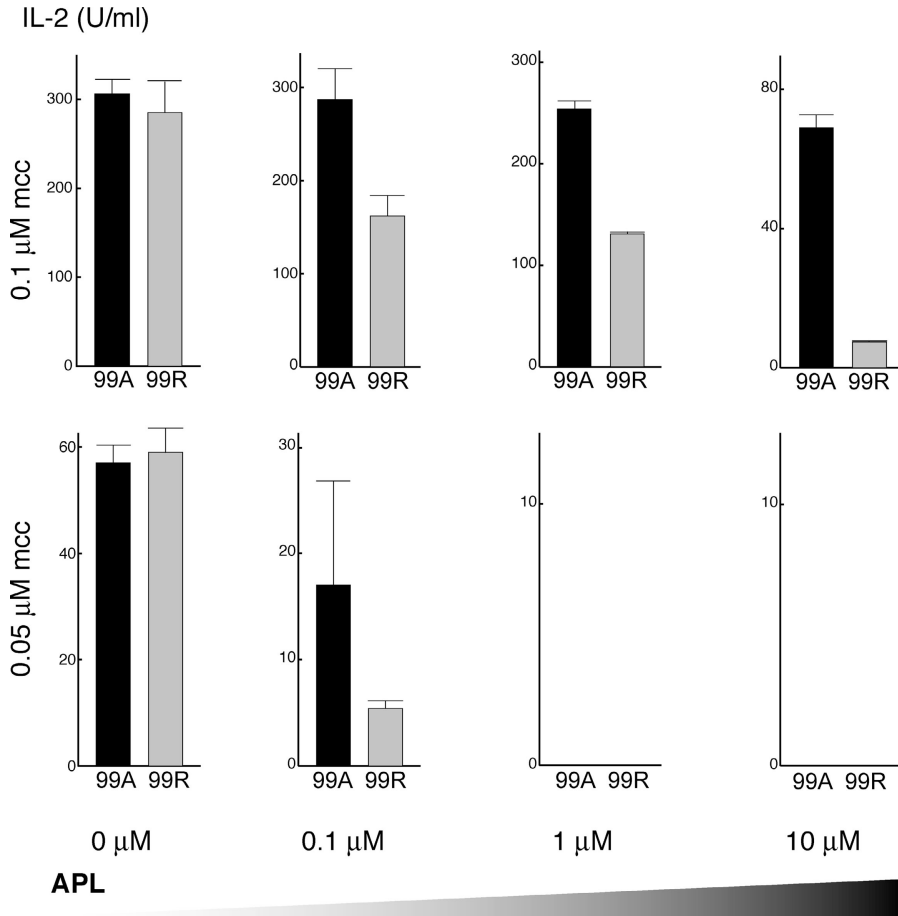


Figure 5. **Antagonist peptides can block T cell effector function at limiting agonist densities.** 5C.C7 T cell blasts were incubated with CH27-ICAM-GFP B cells with the indicated peptide concentrations for 56 h, after which IL-2 levels were quantified by ELISA and normalized to recombinant murine IL-2 standards. For the ratios shown in the two bottom right panels, and at 0.01 μM MCC and lower, no IL-2 above background (assay sensitivity is to 1–10 U/ml range) could be detected. Pairwise comparisons at 0.1, 1, and 10 μM APL and 0.1 μM MCC (top rightmost three graphs) are significant, with  $P < 0.05$  by *t* test. The top right graph features the same peptide ratio as in the microscopy experiments represented by Fig. 4 b. Results are representative of two independent experiments.

### ICAM-1 density and LFA-1 engagement

The initial high intensity ICAM-1 engagement was indicative of efficient LFA-1 binding, likely through avidity up-regulation and mobilization at the interface. To determine the extent of LFA-1 engagement, we quantified the ICAM-1 molecular density in contacts formed in these experiments. Surprisingly, we found that the ICAM-1 density in the sickle-like patterns initially formed on antagonist-agonist MHC bilayers was very high (Fig. 3 d), comparable to the amount measured for ICAM-1 in mature synapses with agonist-MHC alone (Grakoui et al., 1999). Conversely, on antagonist ligand alone, T cells did not accumulate much ICAM-1 over background, which is consistent with a requirement for TCR signaling through PKC to shift LFA-1 to high affinity (Dustin and Springer, 1989). Over time, the ICAM-1 density decreased as the T cells were anergized, consistent with the change in the ICAM-1 pattern seen when the rightmost panels in Fig. 3 (a and c) are compared. Thus, ICAM-1 density in the T cell contact, which is an accurate indicator of LFA-1 engagement, was elevated to levels seen with agonist alone, indicating that at least this aspect of TCR signaling, namely integrin valency up-regulation, was functioning in the presence of antagonist-MHC. Nonetheless, high-density integrin engagement alone was not sufficient to overcome the attenuation of the stop signal by antagonist TCR ligands.

### Integrin engagement and TCR antagonism in live T–B cell interface

To extend these results to live, costimulation-competent APCs, we used the B cell lymphoma CH27 expressing a GFP-linked ICAM-1 molecule. Consistent with previous results (Wulfing et al., 1998), B cells loaded with the MCC peptide caused T cells to form tight contacts leading to elevated intracellular calcium and the early accumulation of ICAM-1 into a small, dense cluster at the center of the synapse (Fig. 4 a). At this peptide concentration, ~1.5% of the MHCs on the B cell surface are occupied by the peptide as detected with pMHC specific antibody staining (unpublished data). Given the MHC density of 220 per square micron for these cells, this resulted in an average plasma membrane agonist-MHC density of 3 pMHC molecules per square micron, or ~2400 pMHCs per cell. When we diluted the agonist into 100-fold excess of antagonist peptide, resulting in 0.03 agonist pMHC per square micron (~20 per cell), we saw that the T cells were still able to adhere to the APCs, and form flat interfaces and flux calcium, albeit intermittently. Approximately half these contacts showed very little ICAM-1 accumulation over background and correlated with little or no calcium flux (Fig. 4 b, top right). However, most of the T cells that formed productive contacts with elevated calcium accumulated ICAM-1 in asymmetric patterns very similar to the sickle-like ones seen on planar bilayers (Fig. 4 b, bottom left), although the clusters

often appeared as patches of higher intensity arrayed in an elongated shape with positive curvature around the perimeter of the T cell contact rather than the contiguous regions of more uniform intensity on bilayers. Consistent with these observations, we found that at these agonist/antagonist ratios significantly fewer T cells overall were fluxing calcium at any given time (Fig. 4 c).

To look at functional downstream effects in these live cell couples, we quantified IL-2 secretion levels in T cells allowed to react with the same B cells loaded with very small amounts of agonist peptide and different amounts of the APLs 99A or 99R. This approach takes advantage of recent results showing that peptide loading on live CH27 cells is linear down to the range of 0.1–0.05  $\mu\text{M}$  by a direct peptide-labeling method (Irvine et al., 2002). Extrapolating from this study and previous quantification of MCC loading on CH27 (Wulfing et al., 2002), we estimated the agonist pMHC density on the B cell surface as 0.03 per square micron (20 molecules per cell) at 0.1  $\mu\text{M}$  of free MCC and 0.015 per square micron (10 per cell) at 0.05  $\mu\text{M}$  of free MCC. At a density of 0.003 per square micron (2 per cell) at 0.01  $\mu\text{M}$  MCC, near the sensitivity limit of T cells (Irvine et al., 2002), we could not detect any IL-2 secretion (unpublished data). At these low but physiologically relevant levels of antigen, the antagonist 99R reduced IL-2 secretion at 1:100 (same ratio as in Fig. 4 b), 1:10, and even 1:1 ratios to MCC, as compared with the null peptide 99A (Fig. 5). Thus, the aberrant ICAM-1 pattern, as evidenced by decreased calcium signaling and a block in downstream effector functions, also accompanied TCR antagonism in live T cell–APC couples and corroborated our previous findings in the supported lipid bilayer system.

## Discussion

In the experiments described here, we have characterized the effect of antagonist peptides on the formation of the immunological synapse by  $\text{CD4}^+$  effector T cells. We find that synapses that form in the presence of antagonists show marked defects in MHC and ICAM-1 dynamics. Although the precise function of a mature T cell synapse, as defined by a central cluster of TCR/pMHC surrounded by engaged integrins, is not yet understood (Lee et al., 2002a; Zaru et al., 2002), its formation does correlate very well with a robust T cell response. In particular, the density of pMHC in the cSMAC correlates directly with the stability of TCR-ligand binding and the extent of T cell activation (Grakoui et al., 1999). Antagonist peptides alone promote neither MHC clustering (Monks et al., 1998; Grakoui et al., 1999) nor Lck accumulation (Erlich et al., 2002). Here, we find that antagonist peptides nonetheless can interfere with pMHC clustering, reducing T cell proliferation and inducing an anergic state that hinders readhesion to the antigen-presenting membrane. T cells are unable to accumulate antagonist pMHC and exhibit a sickle-shaped pattern of integrin ligand (ICAM-1) engagement. The high ICAM-1 density in these aberrant synapses is consistent with normal LFA-1 valency up-regulation (Hibbs et al., 1991). Despite this apparent activation of LFA-1 through inside-out signaling, the T cells

do not stop on the bilayers, which likely accounts for the shape of the ICAM-1 accumulation at the leading edge. Similarly, we find that live T cell–B cell couples also have a polarized, asymmetric accumulation of ICAM-1 (Fig. 4 b) when antagonists and agonists are present at the T–B cell interface, although in this case the T cells are able to arrest, presumably due to additional ligands on the B cell that are not present on the bilayers. It is also possible that *in vitro* models of cell–cell interaction using cell suspensions on a flat glass surface do not allow sufficient discrimination between slow crawling versus full stop behavior. Our efforts to address this issue through quantifying T cell migration over the B cell surface were confounded by random motion and B cell rotation due to convection currents and the absence of a three-dimensional matrix for cell adhesion and support. The full resolution of this issue awaits an appropriate high resolution *in vivo* imaging model.

The stop signal that is most evident using the two-dimensional system of supported lipid bilayers can be viewed as a model for antigen recognition *in vivo*, which is accompanied by T cell motility arrest in nearly every experimental approach to date. One notable exception is a recent study of naive T cells entering peripheral lymph nodes, which show an initial phase of rapid, “random-walk” migration even in the presence of potent activating signals in the form of antigen-loaded dendritic cells. This phase, lasting several hours, occurs before the T cells settle down to stable, long-lived interactions consistent with the stop signal and presumably involving the formation of a mature synapse (Mempel et al., 2004). The cellular mechanism(s) responsible for the initial refractive phase of high T cell motility in the face of antigen exposure is not known, and evidently not recapitulated in the model systems used in this work. This behavior may be a result of additional cues only present in intact lymph nodes, including pro-migratory factors such as chemokines that have been shown to overcome the stop signal under certain conditions (Bromley et al., 2000). Alternatively, the T cells themselves may be altered in some way due to their recent extravasation through the high endothelial venules, perhaps via metalloprotease-mediated proteolysis of adhesion receptors, and require this initial phase to reexpress surface proteins or signaling intermediates that are necessary for T cell motility arrest.

Current models for TCR antagonism invoke a range of phenomena from kinetic competition to conformational changes in the TCR subunits or negative signal spreading (Sloan-Lancaster and Allen, 1996; Dittel et al., 1999). Several studies using dual TCR expressing T cells to study antagonism (Daniels et al., 1999; Dittel et al., 1999; Stotz et al., 1999; Wang and Grey, 2003) have reported conflicting results. Antagonist peptides can alter tyrosine phosphorylation patterns on the  $\text{CD3}\zeta$  chain (Sloan-Lancaster et al., 1994; Madrenas et al., 1995) although this has not been universally observed (Liu and Vignali, 1999) and its relevance to antagonism has been challenged (Pitcher et al., 2003). Nonetheless, these partially-phosphorylated molecules could inhibit T cell activation. As seen in Fig. 3 c, the ICAM-1 sickle pattern is lost over time with continued exposure to antagonist peptides. Likewise, in our readhesion



assay (Fig. 1 e), T cells on agonist-antagonist bilayers were unable to reestablish a disrupted contact. These findings suggest that continuous engagement by antagonist pMHC creates a pool of inactive TCR that gradually disables the ability of the T cell to respond to agonist ligand.

A subset of peptides that are unable to activate T cells (null peptides) can nonetheless cocluster in the synapse in the presence of agonists and augment T cell activation within a lower range of MHC density (Wulfiging et al., 2002). Null and antagonist versions of TCR ligands both possess weaker binding kinetics and lower half-lives of interaction with the TCR (Lyons et al., 1996; Wu et al., 2002). However, these two types of APL have different effects on TCR signaling and synapse formation when copresented with agonist ligands. In particular, null pMHC complexes have no measurable affinity for their cognate TCR (Lyons et al., 1996; Wu et al., 2002), but clearly do bind as they are recruited into the synapse in a TCR dependent manner (Wulfiging et al., 2002). Furthermore, they clearly do not act as antagonists. We propose that this apparent discrepancy might be best addressed by a kinetic model (Fig. 6), where decreasing the half-life of interaction ( $t_{1/2} = \ln 2/k_{off}$ ) of an agonist ligand would produce effects ranging from reducing the activating potential of the peptide (weak agonist), to creating ligands with antagonist properties, and finally null ligands that may be compatible with TCR-MHC binding but do not engage long enough to signal. Mathematical modeling of receptor engagement in the immunological synapse has shown the importance of kinetic boundary conditions that affect molecular patterning (Lee et al., 2002b). Rapid, transient interactions whose kinetics fit the postulated optimal range for antagonism (Fig. 6) may disrupt the cytoskeletal-driven TCR transport to the center of the synapse that characterizes agonist engagement (Wulfiging and Davis, 1998) hinder CD4-TCR association (Zal et al., 2002) or prevent TCR oligomerization as suggested by the results of Reich et al. (1997). This model also poses the testable prediction that for any given TCR there exists a kinetic half-life window where any ligand falling within this range will behave as a TCR antagonist.

Of the downstream mediators of TCR signaling, the only pathway activated by antagonist peptide ligands alone is reported to be SLP-76 recruitment, followed by Vav phosphorylation, and Rac-1 and JNK activation (Huang et al., 2000b). ZAP-70 and LAT are not phosphorylated and there is no clustering of PKC $\theta$  at the interface (Huang et al., 2000a). In the former report, Vav was found to be activated through Fyn kinase rather than Lck. Because TCR antagonism can occur even in the absence of the CD3 $\zeta$  chain (Liu and Vignali, 1999) and Fyn is predicted to favor interactions with the other ITAMs of the TCR (i.e., those on the CD3 $\delta$ ,  $\gamma$ , and  $\epsilon$  chains), perhaps antagonists exert their effects primarily through Fyn and the single ITAM-bearing CD3 chains. Thus, it is relevant that Rac-1 phosphorylation can lead to cytoskeletal rearrangement in the T cell (Acuto and Cantrell, 2000). In the presence of antagonist pMHC, asymmetric integrin engagement in the synapse could be due to inopportune Rac-1 activation as Lck and Fyn compete to differentially activate Vav and dictate cytoskeletal re-

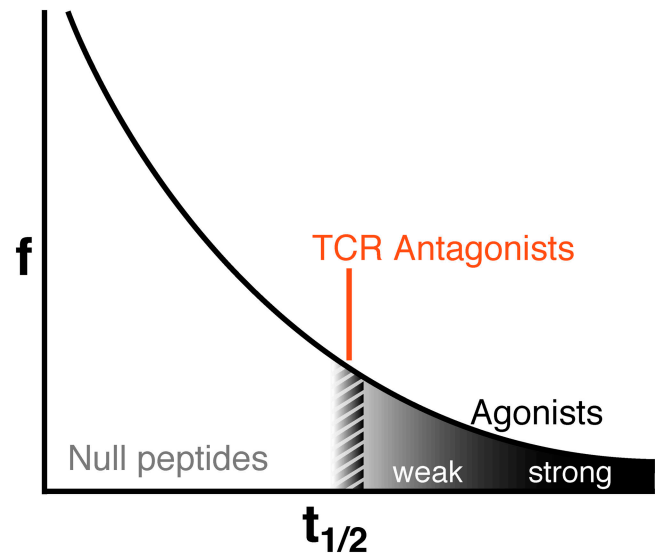


Figure 6. **A model for a narrow kinetic range for TCR antagonism.** The curve represents a hypothetical distribution of pMHC complexes as a group of ligands for a given TCR. Moving from right to left starting with rare agonist peptides that optimally stimulate T cells, as  $t_{1/2}$  (half life of TCR-pMHC interaction) decreases, more peptides show weaker activation potential (increased  $f$ , frequency of peptide), eventually leading to a null phenotype where irrespective of their ability to participate in MHC clustering (Wulfiging et al., 2002), these peptides by themselves do not stimulate T cells. TCR antagonist peptides are postulated to occupy a narrow kinetic window between weak agonists and null ligands, with a sufficient time of interaction for an aberrant or incomplete signal, whereas null peptides do not bind long enough to elicit any signal on their own.

distribution, with Lck favoring a mature synapse and Fyn a more transient interaction coupled with T cell migration. The finding that Vav controls both TCR and integrin clustering through different pathways (a pathway through WASP and an unknown pathway involving Pyk2, respectively) supports this view (Krawczyk et al., 2002).

Similar to our previous work (Wulfiging et al., 2002), another study has described the coclustering of null pMHC with agonist using effector T cells and dendritic cells as APCs (Chmielowski et al., 2002). In contrast, naive T cells “expel” null peptides from the agonist pMHC core, which is postulated to occur via an active mechanism specific to antigen inexperienced cells. Antagonist peptide, but not another null peptide, interferes with this expulsion and causes redistribution across the whole T cell contact. These observations can now be put into context by the work presented here: the exclusion effect in naive T cells is likely due to less efficient null pMHC retention arising from less TCR accumulation at the cSMAC compared with effector T cells. TCR transport deficiency in noneffector T cells is well documented, evidenced by slower or only transient pMHC clustering in naive T cells (Lee et al., 2002a) and thymocytes (Richie et al., 2002). In addition, a recent paper shows that human naive (but not effector) CD8 $^{+}$  T cells are deficient in their ability, independent of antigen, to cluster integrins into a pSMAC ring pattern termed the “presynapse” (Somersalo et al., 2004). Hence the enhanced cytoskeletal activity of effec-

tor T cells would be better able to retain null pMHC corralled at the cSMAC. Antagonists may hinder this effect simply by reducing MHC cluster density, as we show here (Fig. 1 b). The fact that antagonism leads to null pMHC spreading out across the whole interface argues against an active "expulsion process" in naive T cells. If that were indeed the case, antagonists would block this putative process and a central cluster of null pMHC would rather be observed, as with effector T cells. Finally, we note that sickle-like ICAM-1 patterns have also been recently observed in a study of ionomycin-energized Th1 cells (Heissmeyer et al., 2004). The stop signal is similarly compromised, despite some MHC clustering. Hence, that work and ours together support the hypothesis that an aberrant integrin engagement pattern and an abrogated stop signal may comprise novel hallmarks of T cell anergy. In summary, our work complements and extends these studies in quantifying the precise molecular densities of MHC and ICAM-1 and showing how antagonist peptide APLs perturb the density and geometry of molecules at the T cell synapse.

The value of TCR antagonism to a pathogen could be to blunt the immune response toward rare agonist epitopes to defuse T cell help during an infection, especially for small and highly mutagenic viral genomes with a limited number of MHC epitopes for the T cell repertoire. Likewise, HIV can generate Gag epitope variants that act as antagonists to block T cell activation (Klenerman et al., 1994). Our results demonstrate that antagonist peptides, in addition to their role in inhibiting MHC accumulation in the mature synapse, can also disrupt synapse formation by bypassing the stop signal that is normally elicited by antigen engagement, leading to an aberrant integrin pattern and slow but sustained T cell motility. We also show that an increase in integrin avidity alone through inside-out signaling is not sufficient to initiate the T cell stop signal.

## Materials and methods

### Cells, peptides, and proteolipid bilayers

5C.C7 and 2B4 primary T cell blasts were generated by adding 10  $\mu$ M MCC (88–103) peptide to lymph node suspensions from TCR transgenic mice and used 7–12 d later (Grakoui et al., 1999). The CH27 B cell lymphoma expressing ICAM-1-GFP has been described previously (Wulfing et al., 1998). All peptides are single amino acid variants of wild-type MCC (88–103, ANERADLIAYLKQATK) at residue 99K, predicted to be the primary TCR contact, and were purified by HPLC. GPI-linked ICAM-1 and I-E<sup>k</sup> were affinity purified from transfected CHO cells and labeled with Cy5 (Amersham Biosciences) and Oregon green (Molecular Probes) on amine groups as described previously (Bromley et al., 2001b).  $\alpha$ 32-I-E<sup>k</sup> (created by L.C. Wu, Genentech, South San Francisco, CA) features wild-type MCC covalently tethered to the MHC  $\alpha$  chain (Wulfing et al., 2002). GPI-linked proteoliposomes were generated by standard techniques and molecular density was quantified by RIA with appropriate <sup>125</sup>I-labeled antibodies (YN1 for ICAM-1, 14.4.4 for I-E<sup>k</sup>). Proteoliposomes containing Cy3-CD80 and Cy5-CD48 were contributed by S.K. Bromley (Massachusetts General Hospital, Charlestown, MA). G35 and D4 antibodies, specific for peptide-I-E<sup>k</sup>, were used to measure peptide loading efficiency by RIA. His-tagged (6 $\times$  His on COOH terminus of both  $\alpha$  and  $\beta$  chains) I-E<sup>k</sup> (a gift from L. Teyton, The Scripps Research Institute, La Jolla, CA) was produced in S2 insect cells and purified first by anion exchange chromatography (Mono Q; Amersham Biosciences), followed by Ni-NTA agarose (QIAGEN). His-I-E<sup>k</sup> was loaded with CLIP(85–99, KPSVQMRMATPLLMR) before anion exchange to maintain dimer stability during high salt elution; it was exchanged to MCC or its variants after purification. Proteoliposomes with 5% DOGS (1,2-dioleoyl-SN-Glycero-3-[[N(5-amino-1-carboxypentyl) iminodiacetic

acid]succinyl]) in DOPC (1,2-di-oleoyl-SN-glycero-3-ethylphosphocholine; both from Avanti Polar Lipids, Inc.) were used to couple the His-MHC to the bilayer and simultaneously present GPI-linked ICAM-1 and  $\alpha$ 32-I-E<sup>k</sup>. Loading and imaging was done in the presence of 10  $\mu$ M Ni<sup>2+</sup>. Higher maximal densities ( $\sim$ 4000 molecules/ $\mu$ m<sup>2</sup>) and less dependence on free Ni<sup>2+</sup> were obtained with His-I-E<sup>k</sup> than with single-His tagged HLA-A2 (1200–500 molecules/ $\mu$ m<sup>2</sup>), showing that His tag valency plays a role in coupling efficiency to Ni-NTA lipid bilayers. T cells could accumulate Alexa488 (Molecular Probes)-labeled, wild-type MCC agonist loaded His-I-E<sup>k</sup> into a central cluster in the synapse, concomitant with proliferation, indicating that the MHC was mobile and bound in an orientation able to productively interact with TCR.

### T cell functional assays

Proliferation of T cells on bilayers was assayed in a 96-well format. Bilayers were formed from 1  $\mu$ l of vesicle droplets on the bottom of the well, sandwiched by a heat treated (450°C for 8 h) 5-mm coverslip, blocked with 0.2  $\mu$ M filtered BSA solution (2% BSA [Sigma-Aldrich] in 50 mM citrate/phosphate, and 50 mM NaCl) and loaded with peptides overnight at 37°C. After peptide loading, the wells were washed with 10% FCS/RPMI and each glass coverslip flipped in solution to rest with the bilayer side facing up. T cells were added for 48 h at 37°C, followed by 12–16 h of [<sup>3</sup>H]thymidine (Amersham Biosciences) incorporation, transfer to filtermat, and quantification by liquid scintillation (1205 Betaplate; Wallac). IL-2 was quantified from a T cell-B cell coculture assay (relevant peptides added to 1  $\times$  10<sup>5</sup> T and 10<sup>4</sup> B cells/well in 10%FCS/RPMI and incubated at 37°C for 56 h) by a standard sandwich ELISA using epitope-matched antibodies (BD Biosciences) and Europium detection (Victor; Wallac).

### Microscopy and image analysis

Two fluorescent videomicroscopy systems outlined in detail previously (Dustin et al., 1997; Wulfing et al., 2002) were used to collect and process images. The first is a custom inverted microscope (Yona Microscopes) using a 100 $\times$  objective (model Neofluar; Carl Zeiss MicroImaging, Inc.), cooled CCD camera (Photometrics) and IP Lab control software (Signal Analytics). The second is an Axiovert S100TV (Carl Zeiss MicroImaging, Inc. or Universal Imaging Corp.) system using a 63 $\times$  Neofluar objective, 175W Xenon lamp (Sutter Instrument Co.), and an interline cooled CCD-1330-V/HS (Princeton Instruments). Bilayers for imaging were formed in a parallel plate flow chamber (FCS2; Biopetech) or in 8-well chambers (Labtek; Nunc) with 5-mm coverslips. GPI-protein density in contacts from flat-field and background corrected images was quantified as reported previously (Grakoui et al., 1999). ICAM-1 accumulation patterns at the T-B cell interface were generated by three-dimensional reconstruction of background corrected 1  $\mu$ m z-planes collected with a piezo PIFOC motor (Physik Instrumente) mounted underneath the objective, using Metamorph software (Universal Imaging Corp.). Additional image processing used Photoshop, Illustrator (Adobe), and Graphic Converter (Lemke Software). Activation state was monitored by a calcium sensitive dye (Fura-2; Molecular Probes). To judge readhesion efficiency, ice-cold imaging buffer (deficient RPMI [GIBCO BRL], 10% FCS, and 10 mM Hepes) was pulsed into the flow chamber, leading to gradual detachment of the T cells which remained in the field, enabling tracking. As the media warmed back to 37°C, the percentage of T cells previously in contact with the bilayer that could reform a tight contact was scored.

### Online supplemental material

Fig. S1 shows that 99R displays TCR antagonism whether compared with 99A or 99E. The same experimental conditions as in Fig. 5 were used, representative of two experiments. Videos 1–3 correspond respectively to the experiments in Fig. 3, panels a–c. Original image capture was at 30 seconds per frame (shown at 1 second per frame), and each video represents 10 min of imaging. Online supplemental material is available at <http://www.jcb.org/cgi/content/full/jcb.200404059/DC1>.

We are grateful to Shannon Bromley, Luc Teyton, and Lawren Wu for sharing key reagents, and also to Christoph Wulfing, Michelle Krogsgaard, Andrew Girvin, Peter Ebert, Matthew Krummel, and Johannes Huppert for helpful discussions.

This work was supported by the National Institutes of Health and the Howard Hughes Medical Institute.

Submitted: 8 April 2004

Accepted: 6 July 2004

## References

- Acuto, O., and D. Cantrell. 2000. T cell activation and the cytoskeleton. *Annu. Rev. Immunol.* 18:165–184.
- Baker, B.M., S.J. Gagnon, W.E. Biddison, and D.C. Wiley. 2000. Conversion of a T cell antagonist into an agonist by repairing a defect in the TCR/peptide/MHC interface: implications for TCR signaling. *Immunity.* 13:475–484.
- Bertoletti, A., A. Sette, F.V. Chisari, A. Penna, M. Levrero, M. de Carli, F. Fiaccadori, and C. Ferrari. 1994. Natural variants of cytotoxic epitopes are T-cell receptor antagonists for antiviral cytotoxic T cells. *Nature.* 369:407–410.
- Bromley, S.K., and M.L. Dustin. 2002. Stimulation of naive T-cell adhesion and immunological synapse formation by chemokine-dependent and -independent mechanisms. *Immunology.* 106:289–298.
- Bromley, S.K., D.A. Peterson, M.D. Gunn, and M.L. Dustin. 2000. Cutting edge: hierarchy of chemokine receptor and TCR signals regulating T cell migration and proliferation. *J. Immunol.* 165:15–19.
- Bromley, S.K., W.R. Burack, K.G. Johnson, K. Somersalo, T.N. Sims, C. Sumen, M.M. Davis, A.S. Shaw, P.M. Allen, and M.L. Dustin. 2001a. The immunological synapse. *Annu. Rev. Immunol.* 19:375–396.
- Bromley, S.K., A. Iaboni, S.J. Davis, A. Whitty, J.M. Green, A.S. Shaw, A. Weiss, and M.L. Dustin. 2001b. The immunological synapse and CD28-CD80 interactions. *Nat. Immunol.* 2:1159–1166.
- Chmielowski, B., R. Pacholczyk, P. Kraj, P. Kisielow, and L. Ignatowicz. 2002. Presentation of antagonist peptides to naive CD4+ T cells abrogates spatial reorganization of class II MHC peptide complexes on the surface of dendritic cells. *Proc. Natl. Acad. Sci. USA.* 99:15012–15017.
- Daniels, M.A., S.L. Schober, K.A. Hogquist, and S.C. Jameson. 1999. Cutting edge: a test of the dominant negative signal model for TCR antagonism. *J. Immunol.* 162:3761–3764.
- Davis, M.M., J.J. Boniface, Z. Reich, D. Lyons, J. Hampl, B. Arden, and Y. Chien. 1998. Ligand recognition by  $\alpha\beta$  T cell receptors. *Annu. Rev. Immunol.* 16:523–544.
- De Magistris, M.T., J. Alexander, M. Coggeshall, A. Altman, F.C. Gaeta, H.M. Grey, and A. Sette. 1992. Antigen analog-major histocompatibility complexes act as antagonists of the T cell receptor. *Cell.* 68:625–634.
- Dittel, B.N., I. Stefanova, R.N. Germain, and C.A. Janeway. 1999. Cross-antagonism of a T cell clone expressing two distinct T cell receptors. *Immunity.* 11:289–298.
- Dustin, M.L. 2002. Regulation of T cell migration through formation of immunological synapses: the stop signal hypothesis. *Adv. Exp. Med. Biol.* 512:191–201.
- Dustin, M.L. 2003. Coordination of T cell activation and migration through formation of the immunological synapse. *Ann. NY Acad. Sci.* 987:51–59.
- Dustin, M.L., and T.A. Springer. 1989. T-cell receptor cross-linking transiently stimulates adhesiveness through LFA-1. *Nature.* 341:619–624.
- Dustin, M.L., and A.C. Chan. 2000. Signaling takes shape in the immune system. *Cell.* 103:283–294.
- Dustin, M.L., S.K. Bromley, Z. Kan, D.A. Peterson, and E.R. Unanue. 1997. Antigen receptor engagement delivers a stop signal to migrating T lymphocytes. *Proc. Natl. Acad. Sci. USA.* 94:3909–3913.
- Erlich, L.I., P.J. Ebert, M.F. Krummel, A. Weiss, and M.M. Davis. 2002. Dynamics of p56lck translocation to the T cell immunological synapse following agonist and antagonist stimulation. *Immunity.* 17:809–822.
- Grakoui, A., S.K. Bromley, C. Sumen, M.M. Davis, A.S. Shaw, P.M. Allen, and M.L. Dustin. 1999. The immunological synapse: a molecular machine controlling T cell activation. *Science.* 285:221–227.
- Heissmeyer, V., F. Macian, S.-H. Im, R. Varma, S. Feske, K. Venuprasad, H. Gu, Y.-C. Liu, M.L. Dustin, and A. Rao. 2004. Calcineurin imposes T cell unresponsiveness through targeted proteolysis of signaling proteins. *Nat. Immunol.* 5:255–265.
- Hibbs, M.L., H. Xu, S.A. Stacker, and T.A. Springer. 1991. Regulation of adhesion of ICAM-1 by the cytoplasmic domain of LFA-1 integrin  $\beta$  subunit. *Science.* 251:1611–1613.
- Holler, P.D., and D.M. Kranz. 2003. Quantitative analysis of the contribution of TCR/pepMHC affinity and CD8 to T cell activation. *Immunity.* 18:255–264.
- Huang, J., K. Sugie, D.M. La Face, A. Altman, and H.M. Grey. 2000a. TCR antagonist peptides induce formation of APC-T cell conjugates and activate a Rac signaling pathway. *Eur. J. Immunol.* 30:50–58.
- Huang, J., D. Tilly, A. Altman, K. Sugie, and H.M. Grey. 2000b. T-cell receptor antagonists induce Vav phosphorylation by selective activation of Fyn kinase. *Proc. Natl. Acad. Sci. USA.* 97:10923–10929.
- Huppa, J.B., M. Gleimer, C. Sumen, and M.M. Davis. 2003. Continuous T cell receptor signaling required for synapse maintenance and full effector potential. *Nat. Immunol.* 4:749–755.
- Irvine, D.J., M.A. Purbhoo, M. Krogsgaard, and M.M. Davis. 2002. Direct observation of ligand recognition by T cells. *Nature.* 419:845–849.
- Jacobelli, J., S.A. Chmura, D.B. Buxton, M.M. Davis, and M.F. Krummel. 2004. A single class II myosin modulates T cell motility and stopping, but not synapse formation. *Nat. Immunol.* 5:531–538.
- Kersh, G.J., E.N. Kersh, D.H. Fremont, and P.M. Allen. 1998. High- and low-potency ligands with similar affinities for the TCR: the importance of kinetics in TCR signaling. *Immunity.* 9:817–826.
- Kim, M., C. Carman, and T.A. Springer. 2003. Bidirectional transmembrane signaling by cytoplasmic domain separation in integrins. *Science.* 301:1720–1725.
- Klenerman, P., S. Rowland-Jones, S. McAdam, J. Edwards, S. Daenke, D. Lalloo, B. Koppe, W. Rosenberg, D. Boyd, A. Edwards, et al. 1994. Cytotoxic T-cell activity antagonized by naturally occurring HIV-1 Gag variants. *Nature.* 369:403–407.
- Krawczyk, C., A. Oliveira-dos-Santos, T. Sasaki, E. Griffiths, P.S. Ohashi, S. Snapper, F. Alt, and J.M. Penninger. 2002. Vav1 controls integrin clustering and MHC/peptide-specific cell adhesion to antigen-presenting cells. *Immunity.* 16:331–343.
- Krogsgaard, M., N. Prado, E.J. Adams, X.L. He, D.C. Chow, D.B. Wilson, K.C. Garcia, and M.M. Davis. 2003. Evidence that structural rearrangements and/or flexibility during TCR binding can contribute to T cell activation. *Mol. Cell.* 12:1367–1378.
- Kucik, D.F., M.L. Dustin, J.M. Miller, and E.J. Brown. 1996. Adhesion-activating phorbol ester increases the mobility of leukocyte integrin LFA-1 in cultured lymphocytes. *J. Clin. Invest.* 97:2139–2144.
- Lee, K.-H., A.D. Holdorf, M.L. Dustin, A.C. Chan, P.M. Allen, and A.S. Shaw. 2002a. T cell receptor signaling precedes immunological synapse formation. *Science.* 295:1539–1542.
- Lee, S.-J.E., Y. Hori, J.T. Groves, M.L. Dustin, and A.K. Chakraborty. 2002b. Correlation of a dynamic model for immunological synapse formation with effector functions: two pathways to synapse formation. *Trends Immunol.* 23:492–499.
- Liu, H., and D.A.A. Vignali. 1999. Differential CD3 $\zeta$  phosphorylation is not required for the induction of T cell antagonism by altered peptide ligands. *J. Immunol.* 163:599–602.
- Lyons, D.S., S.A. Lieberman, J. Hampl, J.J. Boniface, Y.-H. Chien, L.J. Berg, and M.M. Davis. 1996. A TCR binds to antagonist ligands with lower affinities and faster dissociation rates than to agonists. *Immunity.* 5:53–61.
- Matsui, K., J.J. Boniface, P. Steffner, P.A. Reay, and M.M. Davis. 1994. Kinetics of T-cell receptor binding to peptide/I-Ek complexes: correlation of the dissociation rate with T-cell responsiveness. *Proc. Natl. Acad. Sci. USA.* 91:12862–12866.
- Madrenas, J., R.L. Wange, J.L. Wang, N. Isakov, L.E. Samelson, and R.N. Germain. 1995.  $\zeta$  phosphorylation without ZAP-70 activation induced by TCR antagonists or partial agonists. *Science.* 267:515–518.
- Mempel, T.R., S.E. Henrickson, and U.H. von Andrian. 2004. T-cell priming by dendritic cells in lymph nodes occurs in three distinct phases. *Nature.* 427:154–159.
- Monks, C.R., B.A. Freiberg, H. Kupfer, N. Sciaky, and A. Kupfer. 1998. Three-dimensional segregation of supramolecular activation clusters in T cells. *Nature.* 395:82–86.
- Pitcher, L.A., P.S. Ohashi, and N.S.C. van Oers. 2003. T cell antagonism is functionally uncoupled from the 21- and 23-kDa tyrosine-phosphorylated TCR- $\zeta$  subunits. *J. Immunol.* 171:845–852.
- Purbhoo, M.A., A.K. Sewell, P. Klenerman, P.J. Goulder, K.L. Hilyard, J.I. Bell, B.K. Jakobsen, and R.E. Phillips. 1998. Copresentation of natural HIV-1 agonist and antagonist ligands fails to induce the T cell receptor signaling cascade. *Proc. Natl. Acad. Sci. USA.* 95:4527–4532.
- Rabinowitz, J.D., C. Beeson, C. Wulffing, K. Tate, P.M. Allen, M.M. Davis, and H.M. McConnell. 1996. Altered T cell receptor ligands trigger a subset of early T cell signals. *Immunity.* 5:125–135.
- Reich, Z., J.J. Boniface, D.S. Lyons, N. Borochoy, E.J. Wachtel, and M.M. Davis. 1997. Ligand-specific oligomerization of T cell receptor molecules. *Nature.* 387:617–620.
- Richie, L.I., P.J. Ebert, L.C. Wu, M.F. Krummel, J.J. Owen, and M.M. Davis. 2002. Imaging synapse formation during thymocyte selection: inability of CD3 $\zeta$  to form a stable central accumulation during negative selection. *Im-*

- munity*. 16:595–606.
- Sloan-Lancaster, J., and P.M. Allen. 1996. Altered peptide ligand-induced partial T cell activation: molecular mechanisms and role in T cell biology. *Annu. Rev. Immunol.* 14:1–27.
- Sloan-Lancaster, J., A.S. Shaw, J.B. Rothbard, and P.M. Allen. 1994. Partial T cell signaling: altered phospho- $\zeta$  and lack of zap70 recruitment in APL-induced T cell anergy. *Cell*. 79:913–922.
- Somersalo, K., N. Anikeeva, T.N. Sims, V.K. Thomas, R.K. Strong, T. Spies, T. Lebedeva, Y. Sykulev, and M.L. Dustin. 2004. Cytotoxic T lymphocytes form an antigen-independent ring junction. *J. Clin. Invest.* 113:49–57.
- Stotz, S.H., L. Bolliger, F.R. Carbone, and E. Palmer. 1999. T cell receptor (TCR) antagonism without a negative signal: evidence from T cell hybridomas expressing two independent TCRs. *J. Exp. Med.* 189:253–264.
- Sykulev, Y., Y. Vugmeyster, A. Brunmark, H.L. Ploegh, and H.N. Eisen. 1998. Peptide antagonism and T cell receptor interactions with peptide-MHC complexes. *Immunity*. 9:475–483.
- Takagi, J., B.M. Petre, T. Walz, and T.A. Springer. 2002. Global conformational rearrangements in integrin extracellular domains in outside-in and inside-out signaling. *Cell*. 110:599–611.
- Wang, W., and H.M. Grey. 2003. Study of the mechanism of TCR antagonism using dual-TCR-expressing T cells. *J. Immunol.* 170:4532–4538.
- Wu, L.C., D.S. Tuot, D.S. Lyons, K.C. Garcia, and M.M. Davis. 2002. Two-step binding mechanism for T-cell receptor recognition of peptide–MHC. *Nature*. 418:552–556.
- Wulfing, C., and M.M. Davis. 1998. A receptor/cytoskeletal movement triggered by costimulation during T cell activation. *Science*. 282:2266–2270.
- Wulfing, C., M.D. Sjaastad, and M.M. Davis. 1998. Visualizing the dynamics of T cell activation: intracellular adhesion molecule 1 migrates rapidly to the T cell/B cell interface and acts to sustain calcium levels. *Proc. Natl. Acad. Sci. USA*. 95:6302–6307.
- Wulfing, C., C. Sumen, M.D. Sjaastad, L.C. Wu, M.L. Dustin, and M.M. Davis. 2002. Costimulation and endogenous MHC ligands contribute to T cell recognition. *Nat. Immunol.* 3:42–47.
- Zal, T., M.A. Zal, and N.R.J. Gascoigne. 2002. Inhibition of T cell receptor-coreceptor interactions by antagonist ligands visualized by live FRET imaging of the T-hybridoma immunological synapse. *Immunity*. 16:521–534.
- Zaru, R., T.O. Cameron, L.J. Stern, S. Muller, and S. Valitutti. 2002. Cutting edge: TCR engagement and triggering in the absence of large-scale molecular segregation at the T cell-APC contact site. *J. Immunol.* 168:4287–4291.